

Finite beam curvature related patterns in a saturable medium

Rakesh Kapoor

Center for Advanced Technology, Indore 452 013, India

rkapoor@cat.ernet.in

G.S. Agarwal

Physical Research Laboratory, Navrangpura, Ahmedabad 380 009, India

gsa@prl.ernet.in

Abstract: We study numerically the effects of finite curvature and ellipticity of the Gaussian beam on propagation through a saturating nonlinear medium. We demonstrate generation of different types of pattern arising from the *input phase structure* as well as the phase structure imparted by the nonlinear medium.

©1998 Optical Society of America

OCIS codes: (190.0190) Nonlinear Optics, (330.5000) Pattern

References

1. S. Camacho-Lopez, R. Ramos-Garcia and M.J. Damzen, "Experimental study of propagation of an apertured high intensity laser beam in Kerr active CS₂," *J. Mod. Opt.* **44**, 1671-1681 (1997).
2. G.A. Swartzlander Jr. and C.T. Law, "Optical vortex solitons observed in Kerr nonlinear medium," *Phys. Rev. Lett.* **69**, 2503-2506 (1992).
3. G.A. Swartzlander Jr., D.R. Anderson, J.J. Regan, H. Yin and A.E. Kaplan, "Spatial dark-soliton stripes and grids in self-defocusing materials," *Phys. Rev. Lett.* **66**, 1583-1586 (1991).
4. V. Tikhonenko, J. Christou and B. Luther-Davies, "Three dimensional bright spatial soliton collision and fusion in a saturable nonlinear medium," *Phys. Rev. Lett.* **76**, 2698-2701 (1996).
5. G. Grynberg, A. Maître and A. Petrossian, "Flowerlike patterns generated by a laser beam transmitted through rubidium cell with single feedback mirror," *Phys. Rev. Lett.* **72**, 2379-2382 (1994).
6. W.J. Firth and D.V. Skryabin, "Optical solitons carrying orbital angular momentum," *Phys. Rev. Lett.* **79**, 2450-2453 (1997).
7. The transmission of a Gaussian beam through a Gaussian lens has been shown to yield optical vortices: L.V. Kreminskaya, M.S. Soskin and A.I. Khizhriyak, "The Gaussian lenses give birth to optical vortices in laser beams," *Opt. Commun.* **145**, 377-384 (1998).
8. T. Ackeman, E. Kriege and W. Lange, "Phase singularities via nonlinear beam propagation in sodium vapor," *Opt. Commun.* **115**, 339-346 (1995).
9. J. Courtial, K. Dholakia, L. Allen and M.J. Padgett, "Gaussian beams with very high orbital angular momentum," *Opt. Commun.* **144**, 210-213 (1997).
10. A.E. Siegman, *Lasers* (University Science Books, Mill Valley, California); Chapter 17. Note that we adopt the convention $\exp(ikz - iwt)$ rather than the one used by engineers $\exp(-ikz + iwt)$.
11. R.W. Boyd, *Nonlinear Optics* (Academic Press, New York, 1992) p203.
12. V.Tikhonenko, Y. S. Kivshar, V. V. Steblina and A. A. Zozulya, " Vortex solitons in a saturable optical medium," *J. Opt. Soc. Am. B* **15**, 79-86 (1998).

In recent times, there has been considerable interest[1, 2, 3, 4, 5, 6, 7, 8] in the study of propagation of a beam with certain phase structure, say a vortex structure through a nonlinear medium. The phase structure can give rise to an angular momentum [9] for the beam. It is also known that the phase of the Gaussian beam changes sign [10] as one crosses the focus. It should further be noted that the nonlinear wave equation couples amplitudes and phases, as the nonlinear polarization is in, general complex. Thus, one

would expect that the point at which a beam enters the nonlinear medium would be very important. Besides the sign of the nonlinearity is also important. Keeping this in view, we have carried out a *numerical study* of the propagation of a complex Gaussian beam[10]

$$E = E_0 \exp \left(-\frac{ikx^2}{2q_x} - \frac{iky^2}{2q_y} \right) e^{ikz - i\omega t} \quad (1)$$

through a nonlinear medium with saturable nonlinearity. The complex parameter q in Eq.1 can be written as $q_{x,y} = iz_{Rx,y} - z + z_0$ where $z_{Rx,y} = \pi w_{0x,y}^2 / \lambda$ is the Rayleigh range and the beam waist is located at $z = z_0$. We will throughout assume that the entry face of the nonlinear medium is at $z = 0$. Thus for positive (negative) z_0 the beam's waist is inside (outside before the entry face) the medium and we have a converging (diverging) beam. The saturable nonlinearity will be the one produced by a medium modelled as a collection of two level atoms. Hence, the induced polarization is taken as [11]

$$\begin{aligned} \mathbf{P} &= n \mathbf{d} \left(\frac{\Delta + i}{\Delta^2 + 1 + 2|G|^2} \right) G \\ \Delta &= (\omega_0 - \omega) / \gamma \text{ and } G = \vec{d} \cdot \vec{E} / \hbar \gamma, \end{aligned} \quad (2)$$

where \mathbf{d} is the dipole matrix element for the transition with frequency ω_0 . All frequencies have been scaled with respect to the half width γ of the transition. The sign of the detuning determines whether the nonlinearity is of *focussing* ($\Delta < 0$) or *defocussing* ($\Delta > 0$) type. The parameter $2G$ is the scaled Rabi frequency and n is the density of atoms. On scaling all frequencies with respect to γ and all lengths with respect to l (the length of the medium), the wave equation in slowly varying envelope approximation can be written as

$$\begin{aligned} \frac{\partial G}{\partial \zeta} &= \frac{i}{2kl} \nabla_{\perp}^2 G + \frac{i\alpha l}{2} \left(\frac{\Delta + i}{\Delta^2 + 1 + 2|G|^2} \right) G, \\ \nabla_{\perp}^2 &= \left(\frac{\partial^2}{\partial x_0^2} + \frac{\partial^2}{\partial y_0^2} \right), \\ \zeta &= \frac{z}{l}, x_0 = \frac{x}{l}, y_0 = \frac{y}{l}, \end{aligned} \quad (3)$$

where α is the absorption coefficient at line centre

$$\alpha = \frac{4\pi n d^2 \omega}{\hbar c \gamma}. \quad (4)$$

We will solve Eq.3 subject to the initial condition

$$G = G_0 \exp \left(-\frac{ikx_0^2 l^2}{2q_x} - \frac{iky_0^2 l^2}{2q_y} \right), \quad (5)$$

with complex q .

The pattern formation is very sensitive to the *focussing or defocusing* nature of the medium as well as to the *converging or diverging* nature of the Gaussian beam. The results also depend on the *ellipticity* of the beam. Simulations were done for propagation of a converging elliptic Gaussian beam through a focussing nonlinear medium with $\Delta = -18$ and $\alpha = 300$. The medium thickness was taken to be 7.5cm . The Gaussian beam of $\lambda = 780\text{nm}$. and complex radius of curvatures $q_x = .12 + 2.5\text{cm}$. and $q_y = .21 + 2.5\text{cm}$. was propagated through the medium. To find out the proper aperture size and correct number of iterations the simulations were done with following parameters.

1. The simulations were done first on a 256x256 mesh. The iteration number in each case was decided by observing the convergence of the pattern for different number of iterations. Therefore, the number of iteration for different cases varies from 60 to 100. For converging beams, it was found that the entrance aperture, of four times that of the beam size along both the axes was sufficient for the propagation of 99 percent of the total beam. In case of diverging beams, the aperture size was adjusted to allow 99 percent of the beam through it at the exit plane.

2. In all cases of converging beams, the simulations were repeated with a 512x512 mesh and the aperture was five times of the beam size at the entrance plane. It was found that the results were more or less same as obtained with 256x256 mesh. Therefore, it was decided to use a 256x256 mesh with four times beam size aperture along both the axes.

In successive figures, we present patterns for different cases. All the figures are drawn in pseudo colors. The color shades change from red, yellow, green, blue and magenta for the intensities changing from zero to one. In Figs. 1-6, we present results for the focussing ($\Delta < 0$) medium. Some results for the defocusing medium ($\Delta > 0$) are shown in Fig.7 and Fig. 8. The figures 1-3 (4-6) show the formation of patterns for convergent (divergent) beams. Fig.9 shows the intensity profile and zero lines of the real and imaginary part of the beam at different planes inside the nonlinear medium. This figure shows several *crossings* of the contours of $Re E = 0$, $Im E = 0$ suggesting the generation of *vortices* [7, 12]. It must be added that the propagation of an elliptic beam through a *Kerr* medium has been studied previously [1]. For weak *ellipticity*, the propagation through a saturating medium has also been studied [8]. The flower-like patterns were observed by Grynberg et al [5] who used a feedback mirror. In their case the distance between neighbouring flower petals is roughly determined by the distance of the feedback mirror to the medium. We have presented results in altogether different regimes where the interplay of diffraction and the self-induced phase shift in beam is causing the pattern formation. We also note that for $z_0 \gg z_R$, the incoming beam is almost a plane wave. However the strong nonlinearity is quite sensitive to the small curvature of the wavefront.

In conclusion, we have shown *numerically* how the finite curvature of the input beam can generate very different kind of patterns which depend on the convergent/divergent nature of the beam and on the *focussing or defocusing* characteristics of the medium. The ellipticity of the beam gives rise to optical vortices, which multiply as the nonlinearity of the medium increases.

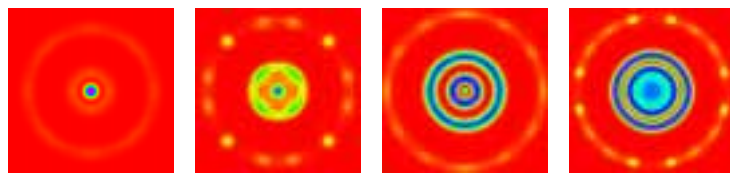


Figure 1. Patterns obtained with propagation of a converging circular-Gaussian beam through a focusing nonlinear medium. The medium was placed at several positions before the beam waist. $\Delta = -18$, $\alpha = 300$, $G_0 = 30$, and $q = (z_0 + .21i)$ cm. The successive frames (from left to right) are for $z_0 = 3.0, 3.5, 4.0$ and 5.0 cm.

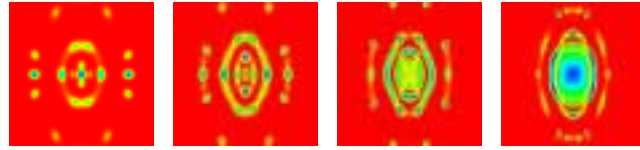


Figure 2. Patterns obtained with propagation of a converging elliptic-Gaussian beam through a focusing nonlinear medium. The medium was placed at several positions before the beam waist. $\Delta = -18$, $\alpha = 300$, $G_0 = 30$, and $q = [z_0 + .12i, z_0 + .21i]$ cm. The successive frames (from left to right) are for $z_0 = 2.5, 3.0, 3.5, 4.0$ and 5.0 cm.

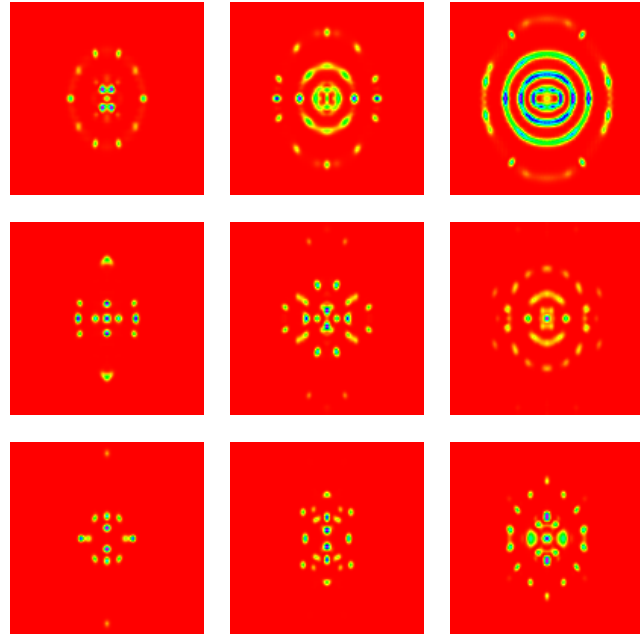


Figure 3. Patterns obtained with propagation of a converging elliptic-Gaussian beam through a focusing nonlinear medium. The medium was placed at before the beam waist. $\Delta = -18$, $q = [z_0 + .12i, z_0 + .21i]$ cm. Patterns were generated for different values of α and G_0 . For different frames the value of $\alpha = 300, 400$, and 500 (from top row to bottom row) and the value of $G_0 = 30, 40$, and 50 (from left column to right column)

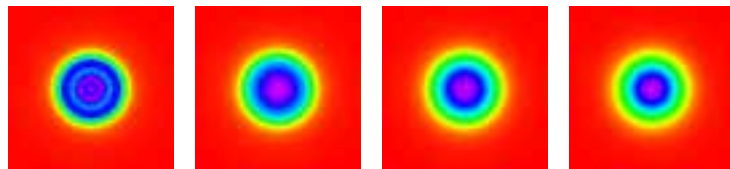


Figure 4. Patterns obtained with propagation of a diverging circular-Gaussian beam through a focusing nonlinear medium. The medium was placed at several positions after the beam waist. $\Delta = -18$, $\alpha = 300$, $G_0 = 30$ and $q = (z_0 + .21i)$ cm. Aperture was 8 times of the input beam size along both the axes. The successive frames (from left to right) are for $z_0 = -3.0, -3.5, -4.0$ and -5.0 cm.

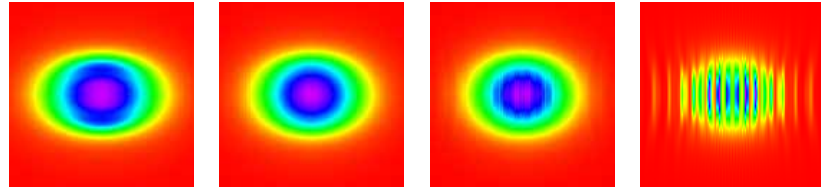


Figure 5. Patterns obtained with propagation of a diverging elliptic-Gaussian beam through a focusing nonlinear medium. The medium was placed at several positions after the beam waist, $\Delta = -18$, $\alpha = 300$, $G_0 = 30$, and $q = [z_0 + .12i, z_0 + .21i]$ cm. Aperture was 8 times of the input beam size along both the axes. The successive frames (from left to right) are for $z_0 = -2.5, -3.0, -3.5, -4.0$ and -5.0 cm.

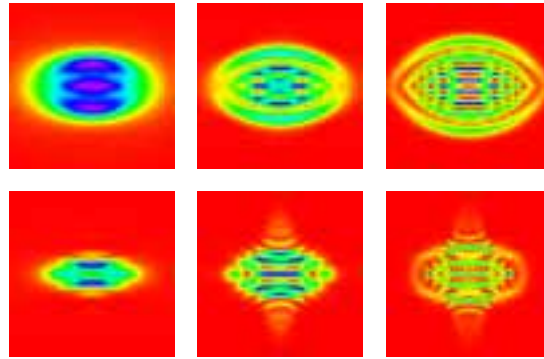


Figure 6. Patterns obtained with propagation of a diverging elliptic-Gaussian beam through a focusing nonlinear medium. The medium was placed at 2.5 cm after the beam waist. $\Delta = -18$, and $q = [-2.5 + .12i, -2.5 + .21i]$ cm. Patterns were generated for different values of α and G_0 . Aperture was 8 times of the input beam size along both the axes. For top row frames $\alpha = 300$, and for the bottom row frames $\alpha = 400$. The value of $G_0 = 30, 40, 50$ (from left to right)

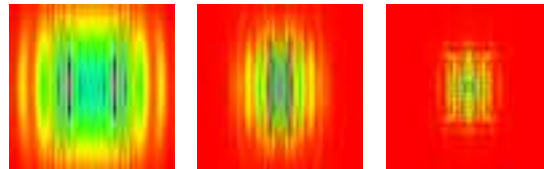


Figure 7. Patterns obtained with propagation of a diverging elliptic-Gaussian beam through a defocusing nonlinear medium. The medium was placed at several positions after the beam waist. $\Delta = -18$, $\alpha = 300$, $G_0 = 30$, and $q = [z_0 + .12i, z_0 + .21i]$ cm. Aperture was 12 times of the input beam size along both the axes. The successive frames (from left to right) are for $z_0 = -3.0, -4.0$ and -5.0 cm.

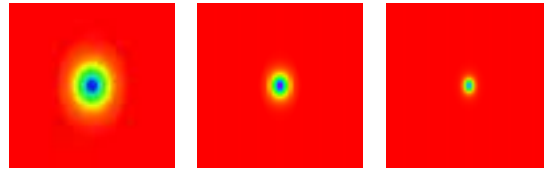


Figure 8. Patterns obtained with propagation of a converging elliptic-Gaussian beam through a defocusing nonlinear medium. The medium was placed at several positions before the beam waist. $\Delta = -18$, $\alpha = 300$, $G_0 = 30$, and $q = [z_0 + .12i, z_0 + .21i]$ cm. Aperture was 12 times of the input beam size along both the axes. The successive frames (from left to right) are for $z_0 = 3.0, 4.0$ and 5.0 cm.

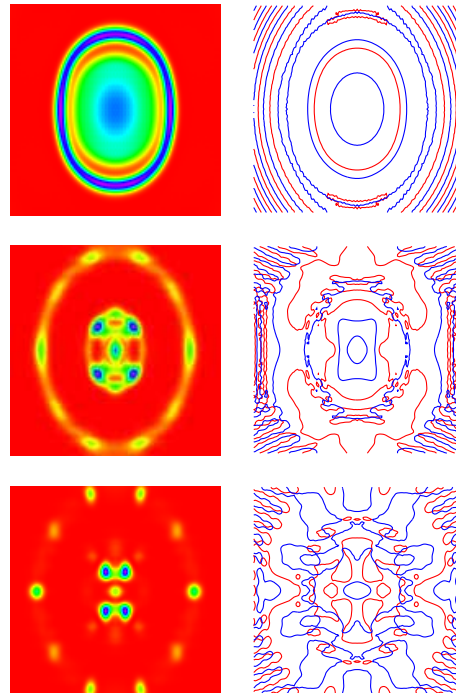


Figure 9. Intensity profiles (left) and zero lines (right) of the real (red line) and imaginary (blue line) part of an elliptic beam propagating through a focusing nonlinear medium. The input beam was a converging beam as the medium was placed at 2.5 cm before the waist of the beam. $\Delta = -18$, $\alpha = 300$, $G_0 = 30$, and $q = [2.5 + .12i, 2.5 + .21i]$ cm. Aperture was 4 times of the input beam size along both the axes. The successive frames were recorded at different positions inside the medium. From top to bottom $z = 4.5, 6.75$ and 7.5 cm.